# Formation mechanisms of oxygen atoms in the $O(^3P_J)$ state from the 157 nm photoirradiation of amorphous water ice at 90 K

Tetsuya Hama,[1] Akihiro Yabushita,[1] Masaaki Yokoyama,[1] Masahiro Kawasaki,[1,a)] and Naoki Watanabe[2]
[1]*Department of Molecular Engineering, Kyoto University, Kyoto 615-8510, Japan*
[2]*Institute of Low Temperature Science, Hokkaido University, Sapporo 060-0819, Japan*

(Received 6 April 2009; accepted 14 July 2009; published online 21 September 2009)

Desorption of ground state $O(^3P_{J=2,1,0})$ atoms following the vacuum ultraviolet photolysis of water ice in the first absorption band was directly measured with resonance-enhanced multiphoton ionization (REMPI) method. Based on their translational energy distributions and evolution behavior, two different formation mechanisms are proposed: One is exothermic recombination reaction of OH radicals, $OH+OH \rightarrow H_2O+O(^3P_J)$ and the other is the photodissociation of OH radicals on the surface of amorphous solid water. The translational and internal energy distributions of OH radicals as well as the evolution behavior were also measured by REMPI to elucidate the roles of $H_2O_2$ and OH in the $O(^3P_J)$ formation mechanisms. © *2009 American Institute of Physics*. [doi:10.1063/1.3194797]

## I. INTRODUCTION

The ultraviolet irradiation on water ice has been studied because of its importance in various areas of science. One of the most intriguing questions is how photoproducts are formed following the photolysis of water ice. The photodissociation of water ice involves two primary processes in the first absorption band at 130–165 nm,

$$H_2O + h\nu \rightarrow H_2 + O(^1D), \tag{1}$$

$$H_2O + h\nu \rightarrow H + OH. \tag{2}$$

In the condensed phase photolysis, the secondary reactions are the sources of photoproducts as well as these two primary processes. For example, the exothermic recombination reaction of two OH radicals, reaction (3), has been well known as a formation mechanism for $H_2O_2$ that is one of the major products in dissociation of low temperature water ice with photons, electrons, or protons,[1–7]

$$OH + OH \rightarrow H_2O_2. \tag{3}$$

Other reaction products from the OH recombination reaction are $H_2O$ and ground state $O(^3P_J)$ atoms, reaction (4). This reaction is well known because of its important role in combustion chemistry and atmospheric relevance at low temperature conditions,[8,9]

$$OH + OH \rightarrow H_2O + O(^3P). \tag{4}$$

Following the ultraviolet photolysis of $H_2O_2$ in various rare-gas matrices at 7.5 K, a complex species, $(H_2O–O)$, was detected, which was produced via the recombination of the OH radicals.[10] The primary formations of $H_2O+O(^1D_2)$ or $O(^3P_J)$ were not established in the photodissociation of gaseous $H_2O_2$ at 124–254 nm.[11] It has not been confirmed whether reaction (4) occurs in the condensed phase photolysis of water ice.

A characteristic phenomenon in the condensed phase is the desorption of products from the secondary reactions of the primary products that are accumulated in the bulk or on the surface. Desorbed products from amorphous solid water (ASW) by photoinduced and electron-stimulated processes were experimentally investigated.[12–20] For example, Kimmel *et al.*[15] reported the low-energy electron-stimulated desorption of O atoms in the $^1D$ and $^3P$ states as well as D atoms from $D_2O$ ice. As reported in the preceding paper, Hama *et al.* have investigated the photoinduced processes of ASW in the first absorption band by direct detection of ejected $O(^1D_2)$ atoms that are produced by two distinct processes: One is the primary unimolecular dissociation of the photoexcited water molecule on the ice surface, reaction (1), and the other process is a secondary bimolecular reaction of hot OH radicals in the electronic ground state. Hot OH radicals are generated from the secondary photolysis of the $H_2O_2$ photoproducts on the ice surface,[21]

$$H_2O + h\nu \rightarrow H + OH, \tag{5}$$

$$OH + OH \rightarrow H_2O_2, \tag{6}$$

$$H_2O_2 + h\nu \rightarrow 2OH, \tag{7}$$

$$OH + OH \rightarrow H_2O + O(^1D). \tag{8}$$

OH radicals which can proceed in endothermic reaction (8) are not produced from the primary photodissociation of $H_2O$ due to the momentum conservation between the photofragments, H and OH. If OH does not have enough energy for reaction (8), $O(^3P_J)$ atoms could be formed via the exothermic reaction (4).

a)Author to whom correspondence should be addressed. Electronic addresses: kawasaki@photon.mbox.media.kyoto-u.ac.jp and kawasaki@moleng.kyoto-u.ac.jp. FAX: +81-75-383-2573.

 

In the present study, using pulsed 157 nm laser radiation the desorption of $O(^3P_J)$ atoms from ASW at 90 K has been directly confirmed by resonance-enhanced multiphoton ionization (REMPI). Translational and internal energies of desorbed $O(^3P_J)$ atoms were measured.

## II. EXPERIMENTAL

### A. Apparatus and preparation of ice films

Experimental details are described elsewhere.[22] ASW was prepared by backfilling deposition of water vapor onto a sapphire disc substrate sputter coated with a thin polycrystalline film of Au(111) at 90 K for 60 min by a pulsed nozzle (General Valve) at rate of 10 Hz and at 20 Torr stagnation pressure of water vapor. In order to spread water vapor all over the chamber, a flat plate was attached in front of the pulse nozzle. The exposure was typically 1500 L (1 L=1 $\times 10^{-6}$ Torr s). This exposure resulted in the formation of 500 monolayers (ML) of $H_2O$ on the substrate if we adopt the reported experimental conversion factor of 1 ML coverage deposition by 3 L exposure.[23]

Unfocused 157 nm laser radiation with a full width at half maximum duration of 10 ns was incident at an angle of about 80° to the surface normal on the ice surface at a fluence $<0.1$ mJ cm$^{-2}$ pulse$^{-1}$. $O(^3P_{J=2,1,0})$ atom products were subsequently ionized at a distance of 4 mm (2 mm for OH) from the substrate surface by the (2+1) REMPI transition via the $O(^3P_J - ^3P_J)$ transition at 225.6–226.4 nm,[24] and collected with a small mass spectrometer aligned perpendicular to the ice surface. OH($v=0$ and 1) products were also detected by REMPI via the $D\,^2\Sigma^-(v'=0) \leftarrow X\,^2\Pi(v''=0)$ at 243.5–245.0 nm and the $3\,^2\Sigma^-(v'=0) \leftarrow X\,^2\Pi(v''=1)$ transitions at 237.5–237.7 nm, respectively.[25] The REMPI transition strength data are obtained from Greenslade *et al.*[25] The delay $t$ between the photolysis and REMPI laser pulses was varied with a delay generator to allow investigation of the flight times of the photoproducts. Three types of ice samples, fresh ASW, ASW after 157 nm photoirradiation for 30 min, and fresh $H_2O_2$ on ASW, were prepared. The surface of fresh ASW was kept fresh for laser irradiation by expanding water vapor to the ASW surface by a pulsed nozzle at a rate of 10 Hz. The duration of the $H_2O$ pulse was about one millisecond. During this exposure, the chamber pressure was increased up to $5 \times 10^{-7}$ Torr. For the concentrated $H_2O_2$ photolysis experiments, a commercially available $H_2O_2$ solution (30%) was concentrated in a glass container by vacuum distillation and the $H_2O_2/H_2O$ vapor was deposited on the gold substrate. The exposure of the codeposited $H_2O_2/H_2O$ mixture on ASW was $<8$ L for 330 s duration at 90 K. Fresh surfaces of cocondensed $H_2O_2$ were prepared as described above. The photolysis experiments were performed at 90 K.

### B. Simulation of time-of-flight spectra of photoproducts

The measured time-of-flight (TOF) spectra were fitted with one or more flux-weighted Maxwell–Boltzmann (MB) distributions defined by a translational temperature $T_{trans}$. Details regarding the simulation of such TOF spectra have been reported previously.[22] The TOF spectrum $S(a_i, t, T_{trans})$ was fitted with a combination of the MB distributions defined by the temperature $T_{trans}$. The coefficient $a_i$ is used for the relative population of each MB distribution,

$$S(a_i, t, T_{trans}) = \Sigma a_i S_{MB}(t, T_{trans}), \tag{9}$$

$$S_{MB}(t, r) = r^3 t^4 \exp[-mr^2/2k_B T_{trans} t^2], \tag{10}$$

$$P_{MB}(E_t) = (k_B T_{trans})^{-2} E_t \exp[-E_t/k_B T_{trans}], \tag{11}$$

where $r$ is a flight length for the photofragment. The MB distribution $P_{MB}(E_t)$ as a function of translational energy $E_t$ is characterized by the averaged translational energy, $\langle E_t \rangle = 2k_B T_{trans}$, where $k_B$ is the Boltzmann constant.[26] Conversion from the energy distribution to the TOF distribution was performed using the Jacobian listed by Zimmerman and Ho.[27]

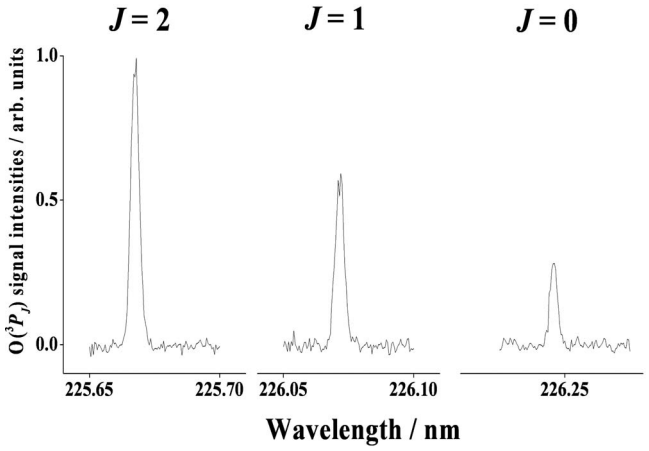


FIG. 1. REMPI excitation spectra of the $O(^3P_J \leftarrow ^3P_J)$ transition from the 157 nm photodissociation of fresh ASW at 90 K. TOF=2.5 $\mu$s.

## III. RESULTS

### A. TOF spectra of $O(^3P_J)$

Figure 1 shows REMPI excitation spectra of the $O(^3P_J - ^3P_J)$ transition following the 157 nm photolysis of fresh ASW at a fixed delay of $t=2.5$ $\mu$s. Figure 2 shows typical TOF spectra of $O(^3P_2)$, the lowest spin-orbit energy level, from the 157 nm photodissociation of (a) fresh ASW, (b) ASW after 157 nm photoirradiation for 30 min, and (c) fresh $H_2O_2$ on ASW. These TOF spectra are well reproduced by four MB distributions with $T_{trans}=5000 \pm 1000$ K ($\langle E_{trans} \rangle = 19.9 \pm 4.0$ kcal/mol), $1300 \pm 200$ K ($5.2 \pm 0.8$ kcal/mol), $300 \pm 100$ K ($1.2 \pm 0.4$ kcal/mol), and $100 \pm 20$ K ($0.4 \pm 0.1$ kcal/mol). Table I summarizes the results. The TOF spectra for (a) fresh ASW and (c) fresh $H_2O_2$ on ASW have similar translational distributions, while those for (b) ASW after 157 nm photoirradiation for 30 min without intermissive dosing of water vapor has a different TOF distribution, that is, the contribution of the $O(^3P_2, T_{trans}=5000$ K) atoms for case (b) is larger than that for cases (a) and (c).

Tables II and III summarize the results of TOF measurements for $O(^3P_{J=2,1,0})$ atoms following the 157 nm photodissociation of the two different ice samples; fresh ASW (Table II) and ASW after 157 nm photoirradiation for 30 min with-

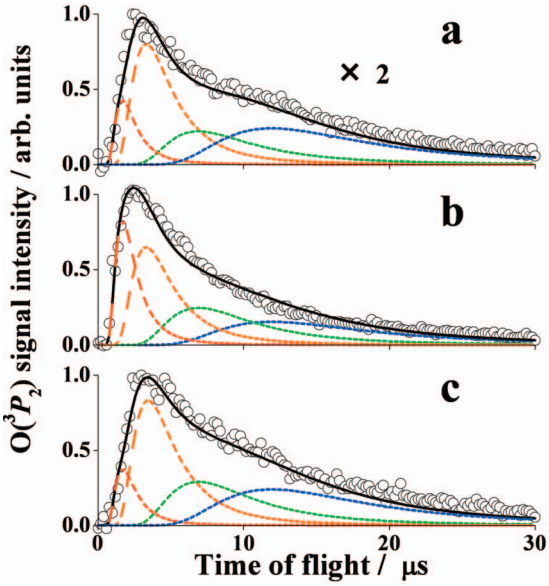


FIG. 2. TOF spectra of $O(^3P_2)$ atoms from the 157 nm photodissociation of (a) fresh ASW at 90 K, (b) ASW after photoirradiation for 30 min, and (c) fresh $H_2O_2$ on ASW. Relative integrated signal intensity ratios and translational temperatures for MB distributions are listed in Table I.

out intermissive dosing of water vapor (Table III), respectively. In both ice samples, the TOF spectra of $O(^3P_{J=2,1,0})$ atoms were reproduced by four MB distributions with $T_{trans}=5000\pm1000$, $1300\pm200$, $300\pm100$, and $100\pm20$ K. The spin-orbit energy level is in the order of $J=0$ (0.65 kcal/mol) $>J=1$ (0.45 kcal/mol) $>J=2$ (0 kcal/mol). The Boltzmann temperatures of the spin-orbit levels, $T_{so}$, for the four translational temperature components are also listed in Table II for fresh ASW and Table III for ASW after 157 nm photoirradiation. As shown in the tables, (a) as a whole, $T_{so}$ for fresh ASW (600 K) and the photoirradiated ASW (1000 K) are not the same, suggesting the different sources of O atoms for ASW after 157 nm photoirradiation, and (b) $T_{so}$ for the lower $T_{trans}$ component is lower, suggesting the lower $T_{trans}$ component is relaxed in the $J$ distribution.

### B. $O(^3P_2)$ signal intensity change as a function of 157 nm photoirradiation time

To verify the origin of the $O(^3P_J, T_{trans}=5000$ K) atom, the time evolution curve of the $O(^3P_2)$ atom was measured as a function of 157 nm irradiation time for the TOF components at $t=1.5$ $\mu$s. Figure 3 shows the results, and the previously reported and presently measured time evolution data for the $R(1)+R(5)$ line of $OH(v=0)$ due to the $H_2O_2$ photoproduct on the 157 nm photoirradiated ASW surface are also plotted, which reflects the concentration of $H_2O_2$ on the ice surface.[7] The appearance behavior of the $O(^3P_2)$ signal in the initial irradiation time ($\sim$600 s) is not in accordance with that of $H_2O_2$ photoproduced via reaction (7). The fact that $O(^3P_2)$ evolves faster than $H_2O_2$ may suggest the other source for the $O(^3P_2)$ atom formation.

### C. OH formation following the 157 nm photolysis of ASW

Formation of the translationally and internally excited OH in the 157 nm photolysis of ASW was confirmed, observing the REMPI signals of $OH(v=0$ and 1).[28] Details of the results were described before.[28] Here in brief, Fig. 4(a) shows the $D\,^2\Sigma^-(v'=0)\leftarrow X\,^2\Pi(v''=0)$ REMPI spectrum of $OH(v=0)$ and Fig. 4(b) shows the mixed band REMPI spectra of OH $D\,^2\Sigma^-(v'=1)\leftarrow X\,^2\Pi(v''=0)$ and $3\,^2\Sigma^-(v'=0)\leftarrow X\,^2\Pi(v''=1)$ from the 157 nm photolysis of fresh ASW at 90 K. The population ratio of $v=1/v=0$ was estimated to be $0.2\pm0.1$ by spectral simulation [Fig. 4(d)] and REMPI transition strength data by Greenslade *et al.*[25] The OH signal intensities from ASW after photoirradiation and fresh $H_2O_2$ on ASW became both 1.5–2.0 times stronger than that from fresh ASW because OH radicals were produced following the photolysis of $H_2O_2$ as well as $H_2O$.

## IV. DISCUSSION

### A. Formation of $O(^3P_J)$ atoms via recombination reactions of OH radicals

#### 1. Fresh ASW

The photodissociation of water ice in the first continuum involves two primary processes, that is, reactions (1) and (2). The quenching of $O(^1D_2)$ atoms generated from reaction (1) to its ground state, $O(^3P_J)$, is unlikely since $O(^1D_2)$ atoms easily react with water molecules to produce two OH radicals or $H_2O_2$ by collisions.[29–31] Following the ultraviolet photolysis of $H_2O_2$ in various rare-gas matrices at 7.5 K, the complex, $(H_2O-O)$, was formed from the recombination reaction of OH photoproducts.[10] Hama *et al.* reported evidences for reaction (8), that is, secondary $O(^1D_2)$ formation via the endothermic recombination of hot OH radicals. Based

TABLE I. Contributions (%) of translational temperature components for each ice sample and relative integrated TOF signal intensities of $O(^3P_2)$ atoms.

| | $T_{trans}$ (K) | | | | Relative integrated TOF signal intensity[a] |
|---|---|---|---|---|---|
| | 5000 | 1300 | 300 | 100 | |
| Fresh ASW[b] | 10 | 36 | 20 | 34 | 1 |
| ASW after photoirradiation[c] | 20 | 32 | 24 | 24 | $1.6\pm0.4$ |
| Fresh $H_2O_2$ on ASW | 8 | 36 | 24 | 32 | $2.0\pm0.4$ |

[a]Integrated TOF signal intensities are relative to fresh ASW sample.
[b]ASW stands for amorphous solid water at 90 K.
[c]After 30 min photoirradiation at 157 nm.

TABLE II. Contributions (%) of translational temperature components for each spin orbit $J$ level, relative integrated TOF signal intensities of $O(^3P_J)$ atom products, and the Boltzmann temperatures of the spin-orbit levels, $T_{so}$, for each translational temperature component. The sample ice is fresh ASW.

| | $T_{trans}$ (K) | | | | |
|---|---|---|---|---|---|
| $J$ | 5000 | 1300 | 300 | 100 | Relative integrated TOF signal intensity[a] |
| 2 | 10 | 36 | 20 | 34 | 1 |
| 1 | 12 | 44 | 22 | 22 | $0.35 \pm 0.04$ |
| 0 | 12 | 54 | 24 | 10 | $0.12 \pm 0.04$ |
| $T_{so}$ (K) | …[b] | 1900 | 900 | 200 | 600 |

[a]Integrated TOF signal intensities are relative to $J=2$.
[b]$T_{so}$ could not be characterized because of the weak signal intensity.

on the present results for fresh ASW, $O(^3P_J)$ is formed via exothermic recombination of OH radicals following the primary photodissociation of $H_2O$,

$$H_2O(ads) + h\nu(157\ nm) \rightarrow H(i) + OH(i), \quad (12)$$

$$OH(i) + OH(i) \rightarrow H_2O(i) + O(^3P) \quad (13)$$

$$\rightarrow H_2O(ads) + O(^3P), \quad (14)$$

$$OH(i) + OH(ads) \rightarrow H_2O(i) + O(^3P) \quad (15)$$

$$\rightarrow H_2O(ads) + O(^3P), \quad (16)$$

where the notation "ads" stands for condensed phase or adsorbed state, and the thermodynamic data for adsorbed species are taken from those for the solid phase. The notation "i" stands for species at the ASW/vacuum interface, and for these species we use the gas phase thermodynamics data.[32,33] The schematic illustrations of reactions (13)–are shown in Fig. 5. Thermodynamic data of these reactions in units of kcal/mol are $E_{avail}(12)=51.2$, $\Delta_r H(13)=-16.9$, $\Delta_r H(14)=-27.5$, $\Delta_r H(15)=-4.0$, and $\Delta_r H(16)=-14.6$, where $E_{avail}$ stands for the maximum available energy for the 157 nm photolysis. The barrier height for reaction (13), $E_{barrier}(13)$, in the gas phase was reported to be 0.1 kcal/mol.[34] Andersson *et al.*[35,36] predicted that the mobility of OH radicals formed in the vacuum ultraviolet photolysis of water ice is low within the ice. However, OH radicals formed in the top 3 ML are quite mobile on top of the surface. On the other hand, Petrik *et al.* reported the low-energy electron-stimulated production of molecular oxygen from thin ASW films and proposed that the electron-stimulated migration of OH or $OH^-$ to the vacuum interface, where they react and produce molecular oxygen, occurs via transport through the hydrogen bond network of the ASW.[17] Both models support that (a) OH products accumulate on the surface of ASW, and (b) the recombination of OH products occurs more readily on the surface of the ASW film compared to the bulk. The vibrational state distribution $v=1/v=0$ of OH($v=0$ and 1) following the 157 nm photolysis of fresh ASW is ~0.2, while in the gas phase the value was reported to be ~1.1 by Lu *et al.*, Hwang *et al.*, and Yang *et al.*[37–39] The reasons for the discrepancy between the condensed and gas phases can be found in differences in the excited state potentials and energy dissipation process.[35,36] These low-energy OH radicals following the photolysis of $H_2O$ produce $O(^3P_J)$ atoms via exothermic reactions (13)–(16).

### 2. Fresh $H_2O_2$ on ASW

As shown in Fig. 2 and Table I, the TOF spectrum for fresh $H_2O_2$ on ASW has a similar translational distribution to that for the fresh ASW, while its signal intensity is doubled. The present experimental results show that the $O(^3P_J)$ atom formation via exothermic recombination of OH radicals since OH radicals are produced following the photodissociation of $H_2O_2$ as well as $H_2O$,

$$H_2O_2(ads) + h\nu(157\ nm) \rightarrow 2OH(i), \quad (17)$$

TABLE III. Contributions (%) of translational temperature components for each spin orbit $J$ level, relative integrated TOF signal intensities of $O(^3P_J)$ atom products, and the Boltzmann temperatures of the spin-orbit levels, $T_{so}$, for each translational temperature component. The sample ice is ASW after 157 nm photoirradiation for 30 min.

| | $T_{trans}$ (K) | | | | |
|---|---|---|---|---|---|
| $J$ | 5000 | 1300 | 300 | 100 | Relative integrated TOF signal intensity[a] |
| 2 | 20 | 32 | 24 | 24 | 1 |
| 1 | 28 | 34 | 26 | 12 | $0.33 \pm 0.12$ |
| 0 | 32 | 38 | 24 | 5 | $0.16 \pm 0.03$ |
| $T_{so}$ (K) | negative[b] | 1900 | 1000 | 200 | 1000 |

[a]Integrated TOF signal intensities are relative to $J=2$.
[b]Negative temperature.

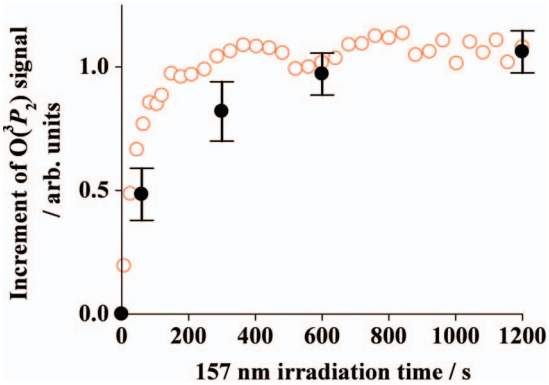


FIG. 3. Time evolution curves of the $O(^3P_2)$ signal at TOF=1.5 $\mu$s as a function of the 157 nm irradiation time (red open circles). The $y$-axis shows increment of the $O(^3P_2)$ signal intensities so that weak signals at $t=0$ s are offset. Previously reported time evolution of OH signal intensity exclusively due to the secondary photolysis of the $H_2O_2$ photoproducts on ASW is represented by the filled circles (Ref. 7).

$$\mathrm{OH(i)} + \mathrm{OH(i)} \rightarrow \mathrm{H_2O(i)} + \mathrm{O}(^3P) \tag{18}$$

$$\rightarrow \mathrm{H_2O(ads)} + \mathrm{O}(^3P), \tag{19}$$

$$\mathrm{OH(i)} + \mathrm{OH(ads)} \rightarrow \mathrm{H_2O(i)} + \mathrm{O}(^3P) \tag{20}$$

$$\rightarrow \mathrm{H_2O(ads)} + \mathrm{O}(^3P), \tag{21}$$

where $E_{\mathrm{avail}}(17)=115.9$ kcal/mol. As reported in the preceding paper by Hama *et al.*, the secondary $O(^1D_2)$ formation occurs via the endothermic recombination of hot OH radicals generated from the photolysis of $H_2O_2$ on the ice surface, reaction (17),[21]

$$\text{hot OH(i)} + \text{hot OH(i)} \rightarrow \mathrm{H_2O(i)} + \mathrm{O}(^1D) \tag{22}$$

$$\rightarrow \mathrm{H_2O(ads)} + \mathrm{O}(^1D), \tag{23}$$

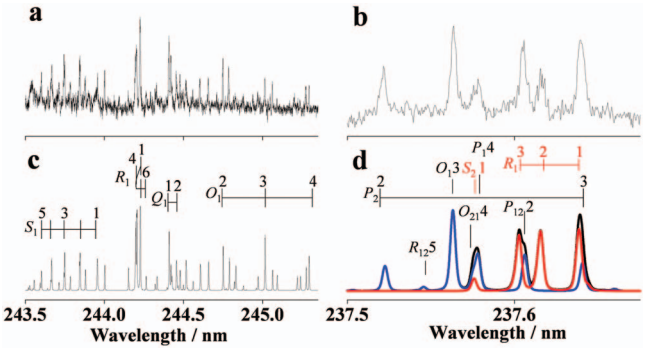


FIG. 4. (a) REMPI excitation spectrum of the OH $D\,^2\Sigma^- \leftarrow X\,^2\Pi$ ($v'=0$, $v''=0$) transition from fresh ASW at 90 K. TOF=1.5 $\mu$s. The arrow indicates the $R(1)+R(5)$ line used for Fig. 2. (b) overlapped REMPI excitation spectra of OH $D\,^2\Sigma^- \leftarrow X\,^2\Pi$ ($v'=1$, $v''=0$) and $3\,^2\Sigma^- \leftarrow X\,^2\Pi$ ($v'=0$, $v''=1$). TOF=1.5 $\mu$s. (c) Simulated OH spectrum assuming a Boltzmann distribution with $T_{\mathrm{rot}}(v=0)=400$ K. (d) Simulated spectrum assuming $T_{\mathrm{rot}}(v=0, \text{blue line})=400$ K and $T_{\mathrm{rot}}(v=1, \text{red line})=300$ K. The black line is a sum of the two simulated spectra. The experimental conditions are the same as for Fig. 1.

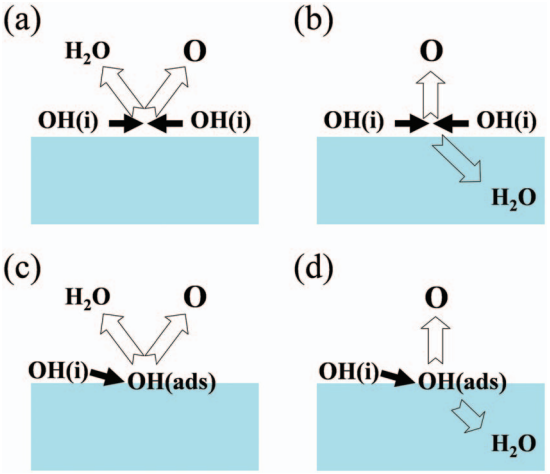


FIG. 5. Schematic illustrations of the collisional recombination reactions of OH radicals on the surface of ice for forming $O(^3P_J)$ atom, (a) reaction (13), (b) reaction (14), (c) reaction (15), and (d) reaction (16). OH(i) stands for OH radical at the ASW/vacuum interface, and OH(ads) stands for adsorbed species.

$$\text{hot OH(i)} + \mathrm{OH(ads)} \rightarrow \mathrm{H_2O(i)} + \mathrm{O}(^1D) \tag{24}$$

$$\rightarrow \mathrm{H_2O(ads)} + \mathrm{O}(^1D). \tag{25}$$

Thermodynamic data in units of kcal/mol are $\Delta_r H(22)=28.3$, $\Delta_r H(23)=17.6$, $\Delta_r H(24)=41.2$, and $\Delta_r H(25)=30.5$.[32,33] OH radicals, which do not have enough energy for reactions (22)–(25), produce $O(^3P_J)$ atoms via the exothermic recombination reactions (18)–(21).

### B. Formation of $O(^3P_J)$ atoms via photodissociation of OH radicals

The $O(^3P_2)$ atoms for ASW after 157 nm photoirradiation for 30 min without intermissive dosing of water vapor have different translational and spin-orbital distributions from those for fresh ASW and fresh $H_2O_2$ on ASW. Thus, the contribution of the $O(^3P_2, T_{\mathrm{trans}}=5000\ \mathrm{K})$ components is larger than the other two TOF spectra, and also the translationally hot $O(^3P_2, T_{\mathrm{trans}}=5000\ \mathrm{K})$ atoms have a higher spin-orbit temperature ($T_{\mathrm{so}}=1000$ K) than that coming from fresh ASW ($T_{\mathrm{so}}=600$ K). These results imply a different origin of the $O(^3P_2, T_{\mathrm{trans}}=5000\ \mathrm{K})$ component.

Gerakines *et al.* reported the evolution of spectral features in $H_2O$ ice photoirradiation and found that OH was observed in ice in the early stage of photoirradiation.[6] Laffon *et al.*[40] reported that a small amount of OH can exist on/in water ice at 90 K. As shown in Fig. 3, the temporal evolution curve for the $O(^3P_2, T_{\mathrm{trans}}=5000\ \mathrm{K})$ signals increases faster than that of $H_2O_2$ accumulated on ASW. A plausible source for this increment in the initial part of the evolution curve of $O(^3P_2)$ atoms would be reaction (26),

$$\mathrm{OH(ads)} + h\nu(157\ \mathrm{nm}) \rightarrow \mathrm{H(i\ or\ ads)} + \mathrm{O}(^3P, T_{\mathrm{trans}}=5000\ \mathrm{K}), \tag{26}$$

where $E_{\mathrm{avail}}(26)=65.7$ kcal/mol for H(i) or 69.9 kcal/mol for H(ads).[32,33] Van Dishoeck and Dalgarno performed theo-

retical *ab initio* calculations on the photodissociation of OH radical. They predicted that the vacuum ultraviolet photodissociation of OH at 152–190 nm would lead only to $O(^3P_J)$ and H atoms.[41,42] After prolonged 157 nm irradiation, the secondary photolysis of the OH adsorbed on the surface of ASW could be a source of $O(^3P_J)$ atoms. A small contribution of the $O(^3P_2, T_{trans}=5000\ K)$ atoms in the TOF spectra for (a) fresh ASW and (c) fresh $H_2O_2$ on ASW is also attributable to the photodissociation OH adsorbed on ice because the intermissive water deposition during the experiment cannot perfectly cover the surfaces.

Figure 2 and Table I show that the $O(^3P_2)$ signal intensity of the TOF spectrum for ASW after 157 nm photoirradiation is about 1.6 times larger than that of fresh ASW. The source for the increment of the $O(^3P_J)$ atoms would be the exothermic recombination of OH radicals following the secondary photodissociation of the $H_2O_2$ photoproduct, as well as the secondary photolysis of the OH adsorbed on the surface of ASW. In fact, our previous work on the photolysis of ASW at 90 K has showed that photogenerated $H_2O_2$ via recombination reaction (3) of OH accumulates on the outermost layer of water ice by prolonged irradiation on ASW at 157 nm.[7]

### C. Other mechanisms for $O(^3P_J)$ formation

When the triplet state of $H_2O$ is photoprepared, $O(^3P_J)$ atom could be produced. Kimmel *et al.*[15] reported the low-energy electron-stimulated desorption of O atoms in the $^1D$ and $^3P$ states from $D_2O$ ice, and that triplet excited states of water can be readily formed leading to $O(^3P_J)$ upon dissociation by electron impact. Kobayashi reported the optical spectra of ASW and crystalline ice and found some evidence for the triplet state in the first absorption band and speculated that the absorption intensity of the triplet state is about 1% of that of the singlet state.[43] The contribution of the triplet process would be small in the photolysis of ASW at 157 nm.

There has been no direct measurement of $O(^3P_J)$ formation via the recombination reaction of H and OH, reaction (27), in the gas phase,

$$H(i) + OH(i) \rightarrow H_2(i) + O(^3P). \quad (27)$$

The rate constant of reaction (27) in the gas phase has been reported based on the reverse process, $H_2+O(^3P)\rightarrow H+OH$, and it is much smaller than that for reaction (13) in the gas phase.[44] Classical molecular dynamics calculations showed H and OH photoproducts recombined to a $H_2O$ molecule following the photolysis of water ice.[35,36] Thus, the contribution of this reaction should be negligible.

The contributions of the other photoproducts on ASW such as $HO_2$ would be small since $HO_2$ is produced from a three-step reaction of $OH+H_2O_2$.

## V. SUMMARY

The production of $O(^3P_J)$ atoms from the 157 nm photodissociation of ASW at 90 K was observed directly using REMPI. After prolonged 157 nm irradiation on the ice, $H_2O_2$ is accumulated on the surface of ice. The $O(^3P_{J=2,1,0})$ atoms are produced mainly via the bimolecular reactions of OH radicals that come from the secondary photodissociation of the accumulated $H_2O_2$. A contribution of the photodissociation of adsorbed OH radical to $O(^3P)+H$ is also observed. Formation of $O(^3P)$ atom from the primary photodissociation of $H_2O$ would be small.

## ACKNOWLEDGMENTS

The authors thank Professor H.-P. Loock of Queen's University for simulation of the rotational spectra of OH radicals and Dr. S. Andersson of SINTEF Materials and Chemistry for fruitful discussions. This work is supported by a grant-in-aid from JSPS (20245005).

[1] W. Zheng, D. Jewitt, and R. I. Kaiser, Astrophys. J. **639**, 534 (2006).
[2] W. Zheng, D. Jewitt, and R. I. Kaiser, Astrophys. J. **648**, 753 (2006).
[3] W. Zheng, D. Jewitt, and R. I. Kaiser, Chem. Phys. Lett. **435**, 289 (2007).
[4] X. Pan, A. D. Bass, J.-P. Jay-Gerin, and L. Sanche, Icarus **172**, 521 (2004).
[5] M. H. Moore, and R. L. Hudson, Icarus **145**, 282 (2000).
[6] P. A. Gerakines, W. A. Schutte, and P. Ehrenfreund, Astron. Astrophys. **312**, 289 (1996).
[7] A. Yabushita, T. Hama, D. Iida, and M. Kawasaki, J. Chem. Phys. **129**, 014709 (2008).
[8] H. Sun, and Z. Li, Chem. Phys. Lett. **399**, 33 (2004).
[9] M.-K. Bahng and R. G. Macdonald, J. Phys. Chem. A **111**, 3850 (2007).
[10] L. Khriachtchev, M. Pettersson, S. Jolkkonen, S. Pehkonen, and M. Rasanen, J. Chem. Phys. **112**, 2187 (2000).
[11] L. J. Stief and V. J. Decarlo, J. Chem. Phys. **50**, 1234 (1969).
[12] M. S. Westley, R. A. Baragiola, R. E. Johnson, and G. A. Baratta, Nature (London) **373**, 405 (1995).
[13] M. S. Westley, R. A. Baragiola, R. E. Johnson, and G. A. Baratta, Planet. Space Sci. **43**, 1311 (1995).
[14] K. I. Öberg, H. Linnartz, R. Visser, and E. F. van Dishoeck, Astrophys. J. **693**, 1209 (2009).
[15] G. A. Kimmel and T. M. Orlando, Phys. Rev. Lett. **75**, 2606 (1995).
[16] G. A. Kimmel, R. G. Tonkyn, T. M. Orlando, Nucl. Instrum. Methods Phys. Res. B **101**, 179 (1995).
[17] N. G. Petrik, A. G. Kavetsky, and G. A. Kimmel, J. Chem. Phys. **125**, 124702 (2006).
[18] A. Yabushita, D. Kanda, N. Kawanaka, M. Kawasaki, and M. N. R. Ashfold, J. Chem. Phys. **125**, 133406 (2006).
[19] A. Yabushita, T. Hama, D. Iida, N. Kawanaka, M. Kawasaki, N. Watanabe, M. N. R. Ashfold, and H. P. Loock, Astrophys. J. Lett. **682**, L69 (2008).
[20] A. Yabushita, T. Hama, D. Iida, N. Kawanaka, M. Kawasaki, N. Watanabe, M. N. R. Ashfold, and H. P. Loock, J. Chem. Phys. **129**, 044501 (2008).
[21] T. Hama, A.Yabushita, M.Yokoyama, M.Kawasaki, and N.Watanabe, J. Chem. Phys. **131**, 114510 (2009).
[22] A. Yabushita, Y. Inoue, T. Senga, M. Kawasaki, and S. Sato, J. Phys. Chem. B **106**, 3151 (2002).
[23] S. Sato, D. Yamaguchi, K. Nakagawa, Y. Inoue, A. Yabushita, and M. Kawasaki, Langmuir **16**, 9533 (2000).
[24] Y. Matsumi, N. Shafer, K. Tonokura, M. Kawasaki, Y.-L. Huang, and R. J. Gordon, J. Chem. Phys. **95**, 7311 (1991).
[25] M. E. Greenslade, M. I. Lester, D. C. Radenovic, A. J. A. van Roij, and D. H. Parker, J. Chem. Phys. **123**, 074309 (2005).
[26] F. M. Zimmermann and W. Ho, J. Chem. Phys. **100**, 7700 (1994).
[27] F. M. Zimmermann and W. Ho, Surf. Sci. Rep. **22**, 127 (1995).
[28] T. Hama, A. Yabushita, M. Yokoyama, M. Kawasaki, and S. Andersson, J. Chem. Phys. **131**, 054508 (2009).
[29] L. Schriver, C. Barreau, and A. Schriver, Chem. Phys. **140**, 429 (1990).
[30] E. J. Dunlea, and A. R. Ravishankara, Phys. Chem. Chem. Phys. **6**, 3333 (2004).
[31] W. Zheng, D. Jewitt, and R. I. Kaiser, Phys. Chem. Chem. Phys. **9**, 2556 (2007).
[32] M. K. Karapet'yants and M. K. Karapet'yants, *Handbook of Thermodynamic Constants of Inorganic and Organic Compounds* (Ann Arbor-Humphrey Science, London, 1970).

[33] A. J. Matich, M. G. Bakker, D. Lennon, T. I. Quickenden, and C. G. Freeman, J. Phys. Chem. **97**, 10539 (1993).
[34] M. Braunstein, R. Panfili, R. Shroll, and L. Bernstein, J. Chem. Phys. **122**, 184307 (2005).
[35] S. Andersson, A. Al-Halabi, G.-J. Kroes, and E. F. van Dishoeck, J. Chem. Phys. **124**, 064715 (2006).
[36] S. Andersson and E. F. van Dishoeck, Astron. Astrophys. **491**, 907 (2008).
[37] I. C. Lu, F. Y. Wang, K. J. Yuan, Y. Cheng, and X. M. Yang, J. Chem. Phys. **128**, 066101 (2008).
[38] D. W. Hwang, X. F. Yang, and X. M. Yang, J. Chem. Phys. **110**, 4119 (1999).
[39] X. F. Yang, D. W. Hwang, J. J. Lin, and X. Ying, J. Chem. Phys. **113**, 10597 (2000).
[40] C. Laffon, S. Lacombe, F. Bournel, and Ph. Parent, J. Chem. Phys. **125**, 204714 (2006).
[41] E. F. van Dishoeck and A. Dalgarno, Astrophys. J. **277**, 576 (1984).
[42] E. F. van Dishoeck and A. Dalgarno, J. Chem. Phys. **79**, 873 (1983).
[43] K. Kobayashi, J. Chem. Phys. **87**, 4317 (1983).
[44] W. Tsang and R. F. Hampson, J. Phys. Chem. Ref. Data **15**, 1087 (1986).